Published in final edited form as:
Circulation. 2005 May 31; 111(21): 2760–2767.

Cardiac Dyssynchrony Analysis Using Circumferential Versus Longitudinal Strain:

Implications for Assessing Cardiac Resynchronization

Robert H. Helm, MD, **Christophe Leclercq, MD**, **Owen P. Faris, PhD**, **Cengizhan Ozturk, MD, PhD**, **Elliot McVeigh, PhD**, **Albert C. Lardo, PhD**, and **David A. Kass, MD**

From the Division of Cardiology, Department of Medicine, Johns Hopkins Medical Institutions, Baltimore, Md (R.H.H., A.C.L., D.A.K.); Department of Biomedical Engineering, Johns Hopkins University, Baltimore, Md (A.C.L., D.A.K.); Department of Cardiology, University of Rennes, Rennes, France (C.L.); and Laboratory of Cardiac Energetics, National Institutes of Health, Bethesda, Md (O.P.F., C.O., E.M.).

Abstract

Background—QRS duration is commonly used to select heart failure patients for cardiac resynchronization therapy (CRT). However, not all patients respond to CRT, and recent data suggest that direct assessments of mechanical dyssynchrony may better predict chronic response. Echo-Doppler methods are being used increasingly, but these principally rely on longitudinal motion (ε_{ll}). It is unknown whether this analysis yields qualitative and/or quantitative results similar to those based on motion in the predominant muscle-fiber orientation (circumferential; ε_{cc}).

Methods and Results—Both ε_{ll} and ε_{cc} strains were calculated throughout the left ventricle from 3D MR-tagged images for the full cardiac cycle in dogs with cardiac failure and a left bundle conduction delay. Dyssynchrony was assessed from both temporal and regional strain variance analysis. CRT implemented by either biventricular (BiV) or left ventricular–only (LV) pacing enhanced systolic function similarly and correlated with improved dyssynchrony based on ε_{cc}-based metrics. In contrast, longitudinal-based analyses revealed significant resynchronization with BiV but not LV for the overall cycle and correlated poorly with global functional benefit. Furthermore, unlike circumferential analysis, ε_{ll}-based indexes indicated resynchronization in diastole but much less in systole and had a lower dynamic range and higher intrasubject variance.

Conclusions—Dyssynchrony assessed by longitudinal motion is less sensitive to dyssynchrony, follows different time courses than those from circumferential motion, and may manifest CRT benefit during specific cardiac phases depending on pacing mode. These results highlight potential limitations to ε_{ll}-based analyses and support further efforts to develop noninvasive synchrony measures based on circumferential deformation.

Keywords

resynchronization therapy; heart failure; bundle-branch block; pacing

Dyssynchronous electrical activation from an intraventricular conduction delay results in discoordinate cardiac contraction and relaxation.[1] Cardiac resynchronization therapy (CRT) including biventricular (BiV) and left ventricular (LV) pacing modes has recently evolved as a new therapeutic modality for heart failure patients with left bundle-branch–type delay

Correspondence to David A. Kass, MD, Ross 835, Johns Hopkins Medical Institutions, 720 Rutland Ave, Baltimore, MD 21205. E-mail dkass@jhmi.edu.

The online-only Data Supplement can be found with this article at http://circ.ahajournals.org/cgi/content/full/CIRCULATIONAHA.104.508457/DC1.

because it enhances ventricular systolic function and energetics,[2] reverses chamber remodeling,[3,4] and improves symptoms, rehospitalization rates, and mortality.[5-7]

Despite its overall efficacy, ≈20% to 30% of patients receiving CRT do not appear to benefit from the therapy,[8] and one concern is that patient selection, which has primarily been based on widening of surface QRS, inadequately identifies chamber dyssynchrony.[9] QRS duration weakly predicts the acute CRT response and has little to no predictive value for chronic improvement.[10-13] Moreover, heart failure patients with normal QRS duration yet mechanical dyssynchrony as determined by echo-Doppler criteria can benefit from chronic CRT.[14]

An alternative to the QRS complex is to examine mechanical dyssynchrony by the analysis of wall motion, and recent studies have shown this to be a better predictor of both acute and chronic improvement from CRT.[15-17] Recent evidence has further suggested that mechanical dyssynchrony predicts worsened cardiac morbidity in heart failure subjects independent of QRS duration and ejection fraction,[18] further highlighting the value of such analysis. Most mechanical dyssynchrony analysis is based on echo-Doppler methods, which in turn are largely derived from longitudinal motion (ε_{ll}) data. This choice of orientation is mainly based on practical grounds given available windows for transducer placement. However, cardiac contraction is principally circumferential (ε_{cc}) (eg, fiber direction), and whether dyssynchrony indexed by circumferential versus longitudinal motion yields similar qualitative, if not quantitative, results remains unknown.

Accordingly, this study compared dyssynchrony measures derived from ε_{ll}- and ε_{cc}-based analyses in an experimental model of heart failure and conduction delay with the use of tagged MRI to provide simultaneous measurements of myocardial strain.[19-21] Our results highlight potentially important qualitative differences in both magnitude and timing of the dyssynchrony measures that should be considered when patients are evaluated. We also explore different methods to synthesize dyssynchrony motion data and reveal added value for metrics that emphasize regional clustering of delayed (versus early) contracting segments.

Methods

Protocol

The experimental model combined radiofrequency ablation of the left bundle branch with 3- to 4-week tachypacing (210 to 250 minutes^{-1} ×3 weeks)-induced heart failure (n=7). Details of the model, as well as limited dyssynchrony analysis based on ε_{cc}-derived measures, have been described previously.[22] This model recapitulates many biochemical, molecular, and structural features relevant to human heart failure, and its mechanical response to resynchronization is analogous to that in patients with dilated cardiomyopathy and conduction delay.[22] Dogs with cardiac dyssynchrony and heart failure were anesthetized, and MRI-compatible pacing leads were positioned in the right atrium (RA), epicardial LV free wall (LV), and right ventricular anteroapex (RV) via median sternotomy. Chamber hemodynamics were measured with an MR-compatible micromanometer (Millar, SPC-350, 5F). Hearts were paced at the RA (dyssynchrony, with left bundle-branch block [LBBB]), LV alone, or LV plus RV (BiV) at 20 beats per minute above intrinsic sinus rate and with AV delay selected to maximize dP/dt_{max} for each pacing configuration. Importantly, tagged cine MRIs in 3 orthogonal directions (ie, 2 axial and 1 longitudinal orientation) were acquired for each pacing protocol and used to derive 3D finite strains. Combining orthogonal tagged MRIs into a 3D strain tensor field markedly reduced errors due to through-plane motion.

Data Analysis

Short- and long-axis tagged MRIs were processed to generate 4D midwall strain tensors from which ε_{cc} and ε_{ll} components were derived as previously described.[23,24] Strain maps for each pacing mode were generated, plotting regional strain for a given heart slice and radial location versus time throughout the cardiac cycle. The time of mitral valve closure defined the zero reference strain. We used aortic valve (AV) closure to define the end of systole. This was based on LV pressure data recorded simultaneously with the acquisition of tagged MR images. Volumetric data were also reconstructed from MRIs; however, under dyssynchronous conditions there was often a plateau in the volume tracing near end-systole so that the exact minimal point was less distinct and often appeared in early diastole. Because end-systolic volumes could not reliably reference AV closure, we used LV pressure tracings instead.

Mechanical dyssynchrony was indexed 3 different ways: temporal uniformity of strain (TUS),[22] regional variance of strain, and regional variance vector (combining both strain magnitude and location) of strain.[25]

First, TUS was determined first by generating a time plot of strain at each of 28 evenly distributed segments (n) around a short-axis slice. Each plot was then subjected to Fourier analysis. If all segments shortened simultaneously (synchronous), the plot appeared as a straight line (power only in the zero-order Fourier term [S_0]; Figure 1A), whereas regionally clustered dyssynchrony (ie, territory of early versus late activation) generated an undulating plot with higher power in the first-order term (S_1; Figure 1A). TUS index reflected the relative first-order power, averaging 4 midchamber slices and time points for the full cycle and selectively for systole and diastole. End-systole was determined from the time of aortic valve closure.

Second, regional variance of strains was determined from the variance of strain magnitude obtained from 28 radially displaced segments for each short-axis section and averaged among slices for each time point. This approach is most similar to many commonly used indexes based on tissue Doppler functional imaging.

Third, regional variance vector of principal strain (RVVPS) was determined first via scaling unit radial vectors, which point in the direction of each segment in a short-axis slice (Figure 1B) by ε_{cc} (or ε_{ll}) magnitude at that location to yield $\vec{\epsilon}_n$. The vectors were then summed to derive a net vector $\vec{v}$ (see Appendix). For synchronous contraction, $\vec{v}$ magnitude was near zero because the radial vectors would cancel out, whereas if a portion of the wall shortened while another stretched, $\vec{v}$ would point toward the shortening. The RVVPS plotted vector magnitude versus time and could be summed to yield an overall index for the full cycle or selectively for systole or diastole.

Statistical Analysis

Data are presented as mean±SEM. Analysis was performed by paired *t* test or 1-way ANOVA with a Tukey test for post hoc comparisons. Computational and statistical analysis was performed with the use of Matlab (MathWorks) and Systat (Systat Software).

Results

Longitudinal Versus Circumferential Motion

Temporal strain maps showing ε_{cc} for each pacing mode are displayed in Figure 2A to 2C. With RA pacing (dyssynchrony, LBBB), there was a zone of late lateral contraction (black arrow) that was fairly uniform from apex to base. The contralateral wall (anterior/posterior septum) showed less net strain and late systolic stretching (gray arrow). With both LV and BiV

pacing, the lateral strain pattern changed. Late lateral contraction is no longer apparent and strain is more homogeneous throughout the myocardium (black arrows, Figure 2B, 2C). Corresponding ε_{ll} maps for the same cardiac cycles are shown in Figure 2D to 2F. The midlevel slices showed a pattern similar to ε_{cc} maps in the dyssynchronous condition (Figure 2D), with a zone of greater late lateral contraction (black arrow) compared with the septal region (gray arrow). However, improved uniformity of ε_{ll} with either LV or BiV pacing was not as apparent as it was with ε_{cc} (black arrows, Figure 2E, 2F). Apical slices typically displayed ε_{ll} shortening patterns that fluctuated and were quite different from those in more basal slices (gray arrows, Figure 2E, 2F).

Correlation of Circumferential- and Longitudinal-Based Dyssynchrony With Global Function

Both BiV and LV pacing similarly enhanced dP/dt_{max} (31.4±9.6% with BiV and 24.7±3.3% with LV; P=0.15) and ejection fraction (18.1±9.7% with BiV and 22.9±9.2% with LV; P=0.4) compared with dyssynchronous baseline (LBBB, atrial pacing), as previously reported in these animals.[22] Furthermore, cardiac dyssynchrony based on TUS for the full cardiac cycle also increased similarly with both CRT modes and correlated with ejection fraction (Figure 3A). In contrast, longitudinal-based motion (ε_{ll} temporal uniformity index) improved only with BiV stimulation; thus, despite global functional improvement with LV-only stimulation, longitudinal analysis did not detect enhanced synchrony (Figure 3B). Similar findings were obtained with the use of dP/dt_{max} as the global systolic function index (ε_{ll} data not shown; ε_{cc} data previously reported[22]).

Summary results for the TUS index are provided in Figure 3C, with a more positive value indicating greater mechanical synchrony. ε_{cc}-based analysis indicated improved synchrony with both LV and BiV pacing during systole, diastole, or the full cycle (all P<0.003). In contrast, ε_{ll}-based analysis showed improved synchrony with BiV, but more in diastole (P<0.001) than systole (P<0.04). With LV-only pacing, improved synchrony was not observed during systole and was borderline significant in diastole (P=0.04).

Dyssynchrony Indexed by Strain Variance and Vector-Spatial Strain Disparities

Because the differences in mechanical dyssynchrony/synchrony reflected by the 2 motion orientations may have depended on how dyssynchrony was assessed, we also determined alternative measures. The first was the spatial strain variance assessed at each time point (Figure 4A, 4B). With the use of ε_{cc}, LBBB hearts displayed a marked rise in dyssynchrony peaking near end-systole, and both LV and BiV stimulation modes reduced evolution (upward slope) and resolution (downward slope) similarly in each cardiac phase (P<0.003). Paired comparisons at defined points in the cardiac cycle (gray highlights) yielded a significant reduction of dyssynchrony with both BiV (P<0.007) and LV (P<0.043) in late systole. In contrast, the same analysis based on ε_{ll} suggested less overall dyssynchrony, and again this was improved by BiV pacing (P=0.019 versus P=0.72 for LV). During diastole, there was resolution of dyssynchrony (downward slope) with both modes (P<0.011). Peak variance at late systole and early diastole was reduced with BiV (P=0.004) but unaltered by LV (P=0.22), and paired comparisons at the same cardiac cycle time points failed to discern differences with either pacing mode compared with baseline dyssynchrony. Thus, this analysis yielded results similar to those from TUS.

A limitation of pure variance-based dyssynchrony measures is that the result is similar regardless of the localization of segments with delayed motion. Having 8 segments with delayed contraction all clustered in 1 region yields the same variance as having them equally dispersed around the heart, yet the impact on global dyssynchrony and function would be very different. To correct for this, we developed a vector-sum index (RVVPS) that weighted strain values by the location of each segment. The resulting RVVPS plots (Figure 4C, 4D) had

patterns similar to those of the strain variance plots but with less intrasubject variability. Corresponding 3D cine images for an example heart are provided (Data Supplement Movies I and II, available online), with the net vector for each short-axis slice displayed and color coded to show changes in its amplitude (dyssynchrony). As with the prior dyssynchrony measures, the evolution and resolution of RVVPS dyssynchrony based on ε_{cc} improved with both pacing modes ($P<0.001$). However, this index revealed less improvement with LV versus BiV during systole and more notably in diastole ($P<0.001$ by ANCOVA for each phase). This disparity was not discerned by the variance method. RVVPS analysis based on ε_{ll} showed little difference among LBBB, LV, or BiV pacing modes during systole ($P>0.179$) and only differences during diastole ($P<0.003$). As with the other indexes, peak RVVPS in late systole and early diastole declined with BiV ($P=0.005$) but not LV ($P=0.3$). Once again, paired comparisons during the cardiac cycle showed no differences.

These temporal analyses are the first to depict the development and resolution of chamber dyssynchrony throughout the cardiac cycle. All 3 dyssynchrony assessments based on longitudinal motion found little to no resynchronization with LV or BiV pacing until diastole and little effect of LV-only pacing regardless of the cycle period. In contrast, circumferential analysis yielded enhanced synchrony with either mode by late systole. Furthermore, temporal-based vector analysis revealed significant differences between LV and BiV pacing with respect to resynchronization effects in systole versus diastole.

Discussion

This study presents the first direct comparison of circumferential strain– and longitudinal strain– based dyssynchrony analysis in a failing heart, contrasting results obtained by 3 independent synchrony measures. There are several important findings. First, longitudinal dyssynchrony indexes have less than half the dynamic range and twice the intrasubject variance of parameters based on circumferential strains, making synchrony/dyssynchrony identification more difficult. Second, on the basis of longitudinal analysis, only BiV but not LV pacing appears to resynchronize the heart, and only in diastole, despite global function being improved similarly by both modes. In contrast, circumferential-based analysis indicates improved synchrony with either mode of CRT during both systole and diastole. Finally, not all dyssynchrony indexes provide identical information, with the vector-based strain variance being most sensitive to temporal differences in synchrony for LV and BiV pacing. These results are important given the growing interest in optimizing CRT utilization based on mechanical dyssynchrony measures and expanding the use of longitudinal-based measurements to this effort.

Myocardial motion is nonisotropic, with a 3-fold difference in amplitude between the principal shortening direction (circumferential, along the dominant fiber orientation) and that perpendicular to it (more longitudinal). As first described by Waldman and Covell,[26] the normal heart displays relatively little longitudinal strain in most myocardial layers. Waldman et al[27] further demonstrated that both orientations do not provide the same information when there are changes in activation due to LV epicardial pacing. Whereas circumferential (or radial) strains displayed a marked change in pattern with LV pacing, with systolic shortening replaced by isovolumic stretch and delayed shortening (eg, similar to lateral contraction with LBBB), the authors found longitudinal strains to be minimally altered. Thus, both timing and shortening pattern were very different as a function of the orientation examined, particularly in the presence of dyssynchrony.

Nearly 20 years later, these prior data have taken on clinical significance because of the development of CRT as a prominent new heart failure therapy and growing appreciation of the value of assessing dyssynchrony to optimize utilization of the therapy. Unlike earlier studies,

we used MRI methodology to provide the full 3D strain field for the heart and to derive global-based dyssynchrony indexes. Furthermore, we obtained such data in a dilated failing heart with an underlying conduction delay to increase similarities to the clinical syndrome. The new data are consistent with earlier work in that longitudinal (versus circumferential) synchrony measures had a narrow dynamic range, did not correlate as well with global function, and did not identify motion abnormalities during systole as much as in diastole. The latter may explain the utility of post-AV shortening in tissue Doppler assessments on the basis of longitudinal motion.[16,17] However, reduced cardiac ejection in dyssynchronous hearts derives from displacement of blood volume from early- to late-activated territory during systole. This is well reflected by circumferential motion and was previously shown with radial motion analysis,[28] but it appears less clear with longitudinal motion. Radial strain analysis would have been interesting to incorporate in the present study; however, there were insufficient MR tags across the myocardium to provide reliable radial motion tracking. Yet, radial strain is more directly related to circumferential strain (eg, circumferential shortening begets radial shortening), unlike longitudinal motion.

There are important similarities and differences between the finite strain analysis used in the present study and longitudinal motion– based Doppler methods used in clinical practice. The most widely used clinical method is tissue Doppler imaging (TDI), which measures ventricular wall velocities relative to the external transducer or mitral annulus and is affected not only by local myocardial deformation (typically longitudinal) but also by overall displacement of the wall due to translational and torsional motion. Attempts to derive measures more specific to myocardial deformation have led to strain rate and strain imaging,[29,30] which have also been useful for dyssynchrony assessment. However, in a recent comparison of the 2 methods, Yu et al[31] found that strain rate imaging analysis had minimal predictive value for chronic reverse remodeling in CRT patients, whereas more general displacement TDI parameters were predictive. Our analysis provides some mechanistic support for these findings, revealing the limitations of a pure longitudinal strain–derived synchrony analysis with respect to its sensitivity and specificity for dyssynchrony.

It should be noted that dyssynchrony examined by longitudinal TDI (tissue velocities) has been shown to decline from CRT with both LV and BiV modes[14,32,33] and during systole[14] and diastole.[15] Furthermore, TDI dyssynchrony analysis has been shown to correlate with chronic echocardiographic benefits in CRT patients in several preliminary studies.[3,15,34] The present findings do not refute such data but rather highlight the likely value of integrating motion from nonlongitudinal orientations (specifically circumferential) into the analyses. As mentioned, TDI-based velocity measurements do this indirectly. From our analysis, more specific longitudinal analyses would seem less optimal, whereas measures that relied more on fiber (circumferential) motion might improve such predictive correlations to an even greater extent.

Recent efforts to index dyssynchrony have principally relied on disparities in the timing of wall motion, generating either a counting index (eg, total number of regions with postsystolic contraction) or variance parameter (statistical variability of time at maximal motion). Neither of these incorporates the spatial placement of these regions, and this may be important to consider. Net mechanical deficiency from discoordinate contraction requires that regions of shortening that are out of phase are geographically clustered together rather than dispersed throughout the wall (Figure 5). Counting and variance-based dyssynchrony measurements cannot differentiate between these 2 conditions. In the present analysis, the variance index had lower sensitivity to detect CRT effects. In contrast, both the temporal variance index and vector index used in this study may distinguish between them because both change only if there are regionally clustered disparities in contraction magnitude, particularly if one region is shortening and the other is stretching. Importantly, our approach can easily be applied to echo-

Doppler analyses as well because such data are generated at multiple sites throughout the ventricular myocardium.

Another novel feature of the present analysis is its depiction of the full time course of dyssynchrony development and resolution, behavior that generally followed a monotonic rise and fall, with peak dyssynchrony near end-systole through mid-diastole. Furthermore, although both BiV and LV-only stimulation enhanced overall circumferential-based resynchronization, cycle phase–specific disparities exist between modes. BiV enhanced synchronization throughout both phases, whereas LV-only stimulation was less efficacious during diastole. This may support the former more widely utilized mode vis-à-vis improving both systolic and diastolic function. This finding is consistent with recent data from our clinical laboratory showing greater effects on diastolic relaxation from BiV over LV pacing in patients with atrial fibrillation and AV conduction block.[33] Determination of dyssynchrony by a variance parameter or at a specific point in the cycle (ie, time of maximal shortening near end-systole) would not have likely revealed such differences.

Recognizing that we used a canine model of dyssynchronous heart failure, some discussion of its clinical relevance is warranted. Although this model mimics many changes observed in human failure and dyssynchrony,[22] it differs in some respects. The model does not result in infarction or fibrosis, and therefore features of this type of failure, in which regional heterogeneity of contraction is produced by tissue damage/fibrosis, timing delay, and their interaction, are absent. However, fiber architecture and the consequent dominant orientation of shortening being circumferential are not changed in ischemic disease, and therefore we believe that our results are applicable to ischemic cardiomyopathies as well. Another difference from clinical CRT implementation is that we used epicardial pacing in both RV and LV. The LV site was similar to that obtained with coronary venous leads (eg, epicardial), whereas the RV site differed because this is usually achieved endocardially. However, given the thin RV wall, it is unlikely that this was a significant factor.

Driven by the demands of CRT, new noninvasive methods to assess cardiac dyssynchrony have been expanding rapidly. Several methods assess radial displacement, such as the septal-posterior wall timing delay method of Pitzalis et al[10] or contrast-echo approach of Kawaguchi et al[28], but most use tissue Doppler with the dominant motion indexed being longitudinal.[34] MRI can provide strains in any orientation, but few clinical studies have used this method to assess mechanical synchrony[35,36] because postprocessing is cumbersome and pacemakers have been considered a contraindication to MRI.[37,38] However, new methods such as 3D-HARP (HARmonic Phase)[39] can provide easy and rapid MRI strain analysis, and evidence now supports the MRI compatibility of modern implantable cardiac devices in patients.[40,41] Thus, clinical applications may be feasible. Regardless of the imaging approach, the greater dynamic range and sensitivity of circumferential (and likely radial) dyssynchrony measures suggest that more robust parameters will be obtained by tracking this motion and will facilitate wider clinical utility and acceptance.

Supplementary Material

Refer to Web version on PubMed Central for supplementary material.

Appendix

Derivation of Normalized TUS

The Fourier decomposition of each component, ε_{cc} and ε_{ll}, of the strain tensor was determined over space (each axial slice) and time. The zero-order component, S_0, of this decomposition was constant and represents perfectly synchronous motion, whereas the first-order component,

S_1, was sinusoidal and represented completely dyssynchronous motion (one wall was contracting while the opposite wall was dilating). The normalized TUS index was calculated as the ratio of the sum of the synchronous segments (S_0) and the sum of the both dyssynchronous (S_1) and synchronous segments over time (t).

$$\mathrm{TUS} = \sqrt{\frac{\sum_t S_0}{\sum_t S_0 + \sum_t S_1}} \tag{1}$$

Thus, a TUS value of 1 indicates perfectly synchronous contraction (in the longitudinal or circumferential direction), whereas a value of 0 indicates completely dyssynchronous contraction.

Derivation of Regional Variance Vector of Principal Strain

A net strain vector, $\vec{v}$, for each short-axis slice (z) and time-step (t_i) was determined by summing the strain vectors at each of 28 evenly distributed sector points.

$$\vec{v}\,(t,z) = \sum_{n=0}^{N} \vec{\epsilon}\,(t,z) \tag{2}$$

The value of the net vector, $\vec{v}$, was scaled by the maximum value of ε_{cc} or ε_{ll} for each dog. The scalar value of the net vector may be summed over z (4 axial slices midway between LV apex and base) to create a time-dependent mean dyssynchrony index.

$$\text{RVVPS Index}\,(t) = \sum_z \vec{v}\,(t,z) \tag{3}$$

This regionally weighted index was plotted versus time throughout the cardiac cycle to assess the mechanical synchrony for all 3 modes of pacing with the use of circumferential and longitudinal strain.

References

1. Leclercq C, Kass DA. Retiming the failing heart: principles and current clinical status of cardiac resynchronization. J Am Coll Cardiol 2002;39:194–201. [PubMed: 11788207]
2. Nelson GS, Berger RD, Fetics BJ, Talbot M, Spinelli JC, Hare JM, Kass DA. Left ventricular or biventricular pacing improves cardiac function at diminished energy cost in patients with dilated cardiomyopathy and left bundle-branch block. Circulation 2000;102:3053–3059. [PubMed: 11120694]
3. Yu CM, Chau E, Sanderson JE, Fan K, Tang MO, Fung WH, Lin H, Kong SL, Lam YM, Hill MR, Lau CP. Tissue Doppler echocardiographic evidence of reverse remodeling and improved synchronicity by simultaneously delayed regional contraction after biventricular pacing therapy in heart failure. Circulation 2002;105:438–445. [PubMed: 11815425]
4. John Sutton MG, Plappert T, Abraham WT, Smith AL, DeLurgio DB, Leon AR, Loh E, Kocovic DZ, Fisher WG, Ellestad M, Messenger J, Kruger K, Hilpisch KE, Hill MR. Effect of cardiac resynchronization therapy on left ventricular size and function in chronic heart failure. Circulation 2003;107:1985–1990. [PubMed: 12668512]
5. McAlister FA, Ezekowitz JA, Wiebe N, Rowe B, Spooner C, Crumley E, Hartling L, Klassen T, Abraham W. Systematic review: cardiac resynchronization in patients with symptomatic heart failure. Ann Intern Med 2004;141:381–390. [PubMed: 15353430]

6. Bristow MR, Saxon LA, Boehmer J, Krueger S, Kass DA, Marco TD, Carson P, DiCarlo L, DeMets D, White BG, DeVries DW, Feldman AM, the Comparison of Medical Therapy, Pacing, and Defibrillation in Heart Failure (COMPANION) Investigators. Cardiac-resynchronization therapy with or without an implantable defibrillator in advanced chronic heart failure. N Engl J Med 2004;350:2140–2150. [PubMed: 15152059]
7. Abraham WT, Fisher WG, Smith AL, Delurgio DB, Leon AR, Loh E, Kocovic DZ, Packer M, Clavell AL, Hayes DL, Ellestad M, Trupp RJ, Underwood J, Pickering F, Truex C, McAtee P, Messenger J, the MIRACLE Study Group. Multicenter InSync Randomized Clinical Evaluation: cardiac resynchronization in chronic heart failure. N Engl J Med 2002;346:1845–1853. [PubMed: 12063368]
8. Kass DA. Ventricular resynchronization: pathophysiology and identification of responders. Reviews Card Med 2003;4:S3–S13.
9. Bleeker GB, Schalij MJ, Molhoek SG, Verwey HF, Holman ER, Boersma E, Steendijk P, Van Der Wall EE, Bax JJ. Relationship between QRS duration and left ventricular dyssynchrony in patients with end-stage heart failure. J Cardiovas Electrophysiol 2004;15:544–549.
10. Pitzalis MV, Iacoviello M, Romito R, Massari F, Rizzon B, Luzzi G, Guida P, Andriani A, Mastropasqua F, Rizzon P. Cardiac resynchronization therapy tailored by echocardiographic evaluation of ventricular asynchrony. J Am Coll Cardiol 2002;40:1615–1622. [PubMed: 12427414]
11. Fauchier L, Marie O, Casset-Senon D, Babuty D, Cosnay P, Fauchier JP. Interventricular and intraventricular dyssynchrony in idiopathic dilated cardiomyopathy: a prognostic study with Fourier phase analysis of radio-nuclide angioscintigraphy. J Am Coll Cardiol 2002;40:2022–2030. [PubMed: 12475464]
12. Bax JJ, Ansalone G, Breithardt OA, Derumeaux G, Leclercq C, Schalij MJ, Sogaard P, John Sutton M. Nihoyannopoulos P. Echocardiographic evaluation of cardiac resynchronization therapy: ready for routine clinical use? A critical appraisal. J Am Coll Cardiol 2004;44:1–9. [PubMed: 15234396]
13. Reuter S, Garrigue S, Barold SS, Jais P, Hocini M, Haissaguerre M, Clementy J. Comparison of characteristics in responders versus nonresponders with biventricular pacing for drug-resistant congestive heart failure. Am J Cardiol 2002;89:346–350. [PubMed: 11809441]
14. Turner MS, Bleasdale RA, Vinereanu D, Mumford CE, Paul V, Fraser AG, Frenneaux MP. Electrical and mechanical components of dyssynchrony in heart failure patients with normal QRS duration and left bundle-branch block: impact of left and biventricular pacing. Circulation 2004;109:2544–2549. [PubMed: 15148267]
15. Sogaard P, Egeblad H, Kim WY, Jensen HK, Pedersen AK, Kristensen BO, Mortensen PT. Tissue Doppler imaging predicts improved systolic performance and reversed left ventricular remodeling during long-term cardiac resynchronization therapy. J Am Coll Cardiol 2002;40:723–730. [PubMed: 12204503]
16. Oguz E, Dagdeviren B, Bilsel T, Akdemir O, Erdinler I, Akyol A, Ulufer T, Gurkan K. Echocardiographic prediction of long-term response to biventricular pacemaker in severe heart failure. Eur J Heart Fail 2002;4:83–90. [PubMed: 11812668]
17. Breithardt OA, Stellbrink C, Kramer AP, Sinha AM, Franke A, Salo R, Schiffgens B, Huvelle E, Auricchio A. Echocardiographic quantification of left ventricular asynchrony predicts an acute hemodynamic benefit of cardiac resynchronization therapy. J Am Coll Cardiol 2002;40:536–545. [PubMed: 12142123]
18. Bader H, Garrigue S, Lafitte S, Reuter S, Jais P, Haissaguerre M, Bonnet J, Clementy J, Roudaut R. Intra-left ventricular electromechanical asynchrony: a new independent predictor of severe cardiac events in heart failure patients. J Am Coll Cardiol 2004;43:248–256. [PubMed: 14736445]
19. O'Dell WG, Moore CC, Hunter WC, Zerhouni EA, McVeigh ER. Three-dimensional myocardial deformations: calculation with displacement field fitting to tagged MR images. Radiology 1995;195:829–835. [PubMed: 7754016]
20. McVeigh ER, Zerhouni EA. Noninvasive measurement of transmural gradients in myocardial strain with MR imaging. Radiology 1991;180:677–683. [PubMed: 1871278]
21. Axel L, Goncalves RC, Bloomgarden D. Regional heart wall motion: two dimensional analysis and functional imaging with MR imaging. Radiology 1992;183:745–750. [PubMed: 1584931]
22. Leclercq C, Faris O, Tunin R, Johnson J, Kato R, Evans F, Spinelli J, Halperin H, McVeigh E, Kass DA. Systolic improvement and mechanical resynchronization does not require electrical synchrony

in the dilated failing heart with left bundle-branch block. Circulation 2002;106:1760–1763. [PubMed: 12356626]

23. Ozturk C, McVeigh ER. Four-dimensional B-spline based motion analysis of tagged MR images: introduction and in vivo validation. Phys Med Biol 2000;45:1683–1702. [PubMed: 10870718]
24. Declerck J, Denney TS, Ozturk C, O'Dell W, McVeigh ER. Left ventricular motion reconstruction from planar tagged MR images: a comparison. Phys Med Biol 2000;45:1611–1632. [PubMed: 10870714]
25. Wyman B, Hunter WC, Prinzen FW, Faris OP, McVeigh ER. Effects of single- and biventricular pacing on temporal and spatial dynamics of ventricular contraction. Am J Physiol 2002;282:H372–H379.
26. Waldman LK, Covell JW. Effects of ventricular pacing on finite deformation in canine left ventricles. Am J Physiol 1987;252(pt2):H1023–H1030. [PubMed: 3578536]
27. Waldman LK, Fung YC, Covell JW. Transmural myocardial deformation in the canine left ventricle. Circ Res 1985;57:152–163. [PubMed: 4006099]
28. Kawaguchi M, Murabayashi T, Fetics BJ, Nelson GS, Samejima H, Nevo E, Kass DA. Quantitation of basal dyssynchrony and acute resynchronization from left or biventricular pacing by novel echo-contrast variability imaging. J Am Coll Cardiol 2002;39:2052–2058. [PubMed: 12084608]
29. Heimdal A, Styolen A, Torp H, Skjaerpe T. Real-time strain rate imaging of the left ventricle by ultrasound. J Am Soc Echocardiogr 1998;11:1013–1019. [PubMed: 9812093]
30. Sutherland GR, Di Salvo G, Claus P, D'hooge J, Bijnens B. Strain and strain rate imaging: a new clinical approach to quantifying regional myocardial function. J Am Soc Echocardiogr 2004;17:788–802. [PubMed: 15220909]
31. Yu C, Fung JW, Zhang Q, Chan C, Chan Y, Lin H, Kum LC, Kong S, Zhang Y, Sanderson JE. Tissue Doppler imaging is superior to strain rate imaging and postsystolic shortening on the prediction of reverse remodeling in both ischemic and nonischemic heart failure after cardiac resynchronization therapy. Circulation 2004;110:66–73. [PubMed: 15197148]
32. Vinereanu D, Bleasdale R, Turner M, Frenneaux MP, Fraser AG. Comparison of left ventricular-biventricular pacing on ventricular synchrony, mitral regurgitation, and global left ventricular function in patients with severe chronic heart failure. Am J Cardiol 2004;94:519–521. [PubMed: 15325945]
33. Hay I, Melenovsky V, Fetics BJ, Judge DP, Kramer A, Spinelli J, Reister C, Kass DA, Berger RD. Acute effects of right-left heart sequential cardiac resynchronization in patients with heart failure, chronic atrial fibrillation, and AV nodal block. Circulation 2004;110:3404–3410. [PubMed: 15557370]
34. Sogaard P, Kim WY, Jensen HK, Mortensen P, Pedersen AK, Kristensen BO, Egeblad H. Impact of acute biventricular pacing on left ventricular performance and volumes in patients with severe heart failure: a tissue Doppler and three-dimensional echocardiographic study. Cardiology 2001;95:175–182.
35. Nelson GS, Curry CW, Wyman BT, Kramer A, Declerck J, Talbot M, Douglas MR, Berger RD, McVeigh ER, Kass DA. Predictors of systolic augmentation from left ventricular preexcitation in patients with dilated cardiomyopathy and intraventricular conduction delay. Circulation 2000;101:2703–2709. [PubMed: 10851207]
36. Zwaneburg JJM, Gotte MJW, Kuijer JPA, Heethaar RM, van Rossum AC, Marcus JT. Timing of cardiac contraction in humans mapped by high-temporal-resolution MRI tagging: early onset and late peak of shortening in lateral wall. Am J Physiol 2004;286:H1872–H1880.
37. Niehaus M, Tebbenjohanns J. Electromagnetic interference in patients with implanted pacemakers or cardioverter-defibrillators. Heart 2001;86:246–248. [PubMed: 11514470]
38. Pinski SL, Trohman RG. Interference in implanted cardiac devices, part II. Pacing Clin Electrophysiol 2002;25:1496–1509. [PubMed: 12418748]
39. Pan L, Lima JA, Osman NF. Fast tracking of cardiac motion using 3D-HARP. Inf Process Med Imaging 2003;18:611–622. [PubMed: 15344492]
40. Martin ET, Coman JA, Shellock FG, Pulling CC, Fair R, Jenkins K. Magnetic resonance imaging and cardiac pacemaker safety at 1.5-Tesla. J Am Coll Cardiol 2004;43:1315–1324. [PubMed: 15063447]

41. Sommer T, Vahlhaus C, Lauck G, von Smekal A, Reinke M, Hofer U, Block W, Traber F, Schneider C, Gieseke J, Jung W, Schild H. MR imaging and cardiac pacemakers: in vitro evaluation and in vivo studies in 51 patients at 0.5 T. Radiology 2000;215:869–879. [PubMed: 10831713]

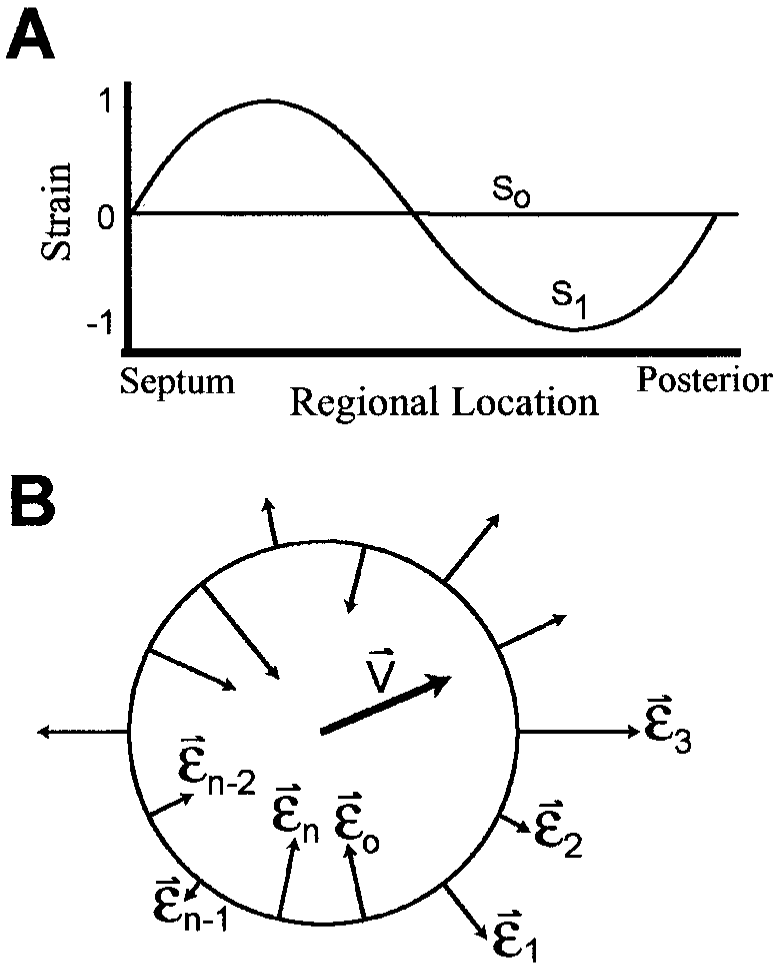

Figure 1.

A, Schematic for determination of TUS dyssynchrony index. Strain is plotted at a given time as a function of spatial location of the segment. Data are processed by Fourier series decomposition. The zero-order (S_0) and first-order (S_1) terms are shown plotted vs spatial position. A perfectly synchronous heart would appear as a straight line (solely S_0 term), whereas one that was perfectly dyssynchronous would appear as a sinusoid (S_1 term). The index relates the relative power of these 2 terms (Appendix). B, Schematic for calculating vector-strain index. For a given short-axis slice, strains at each segment are determined, and this value was multiplied by a unit vector pointing in the direction of the segment. The vectors are then added, and the sum V reflects the primary orientation and magnitude of contraction. If all segments contract at the same time, the magnitude of V is zero; with increasing dyssynchrony of contraction, the magnitude of V increases.

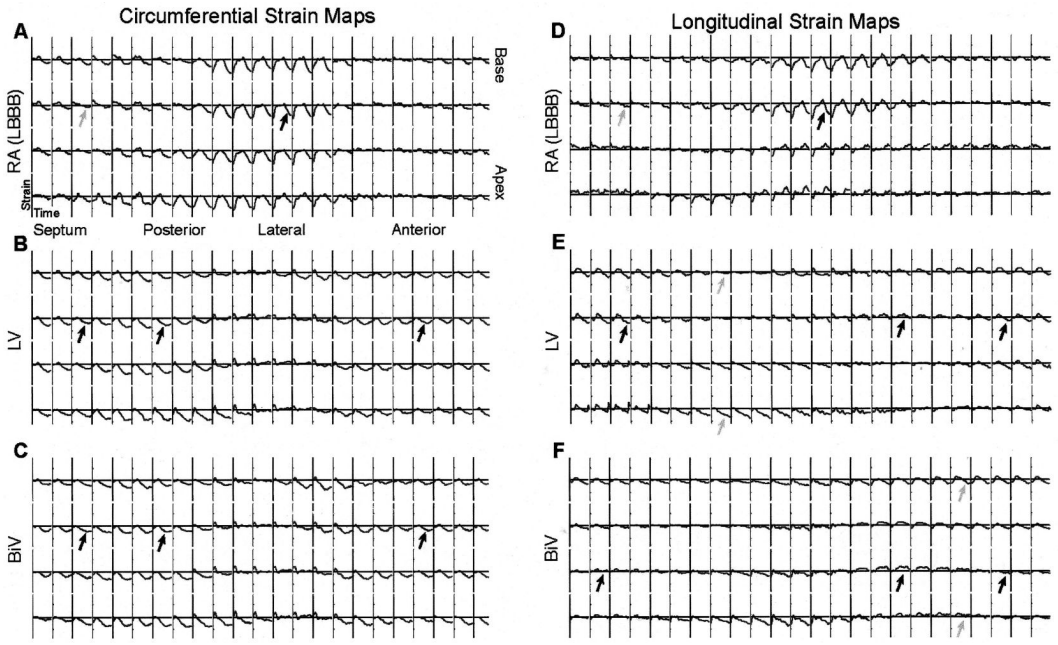

Figure 2.

Temporal-spatial maps of ε_{cc} and ε_{ll} for RA (LBBB), LV, and BiV pacing modes. Each subplot within a map shows the time-dependent (*x* axis) circumferential or longitudinal (*y* axis) motion at a spatial point around the LV. A zone of increased ε_{cc} and ε_{ll} strain is demonstrated in the lateral wall of the RA (LBBB) paced heart (A, D). Both LV and BiV modify this lateral wall strain pattern, although the effects are less pronounced with ε_{ll} (E, F) than with ε_{cc} (B, C). See text for details.

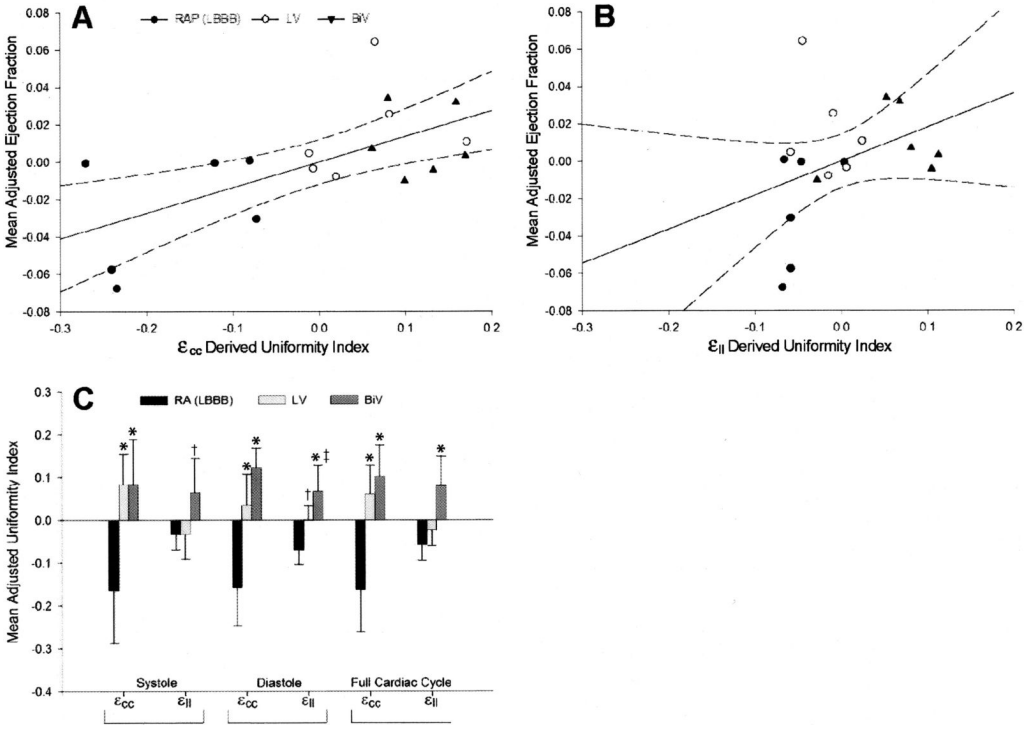

Figure 3.

Comparison of full-cycle ε_{cc}- and ε_{ll}-derived temporal uniformity in the LBBB dyssynchrony model. With both LV and BiV pacing, the ε_{cc}-derived uniformity index positively correlates with enhanced EF (A). However, unlike ε_{cc}, ε_{ll} uniformity is not enhanced with LV pacing despite improved hemodynamic function (B). The dynamic range of ε_{ll} uniformity is much less than that of ε_{cc} uniformity. Ejection fraction is adjusted according to its mean value for each respective animal. C, ε_{cc} and ε_{ll} temporal uniformity in the LBBB dyssynchrony model averaged over systole, diastole, and the full cardiac cycle. *P<0.003, †P=0.04 vs RA (LBBB) dyssynchronous baseline; ‡P=0.05 vs BiV. Data are mean±SEM.

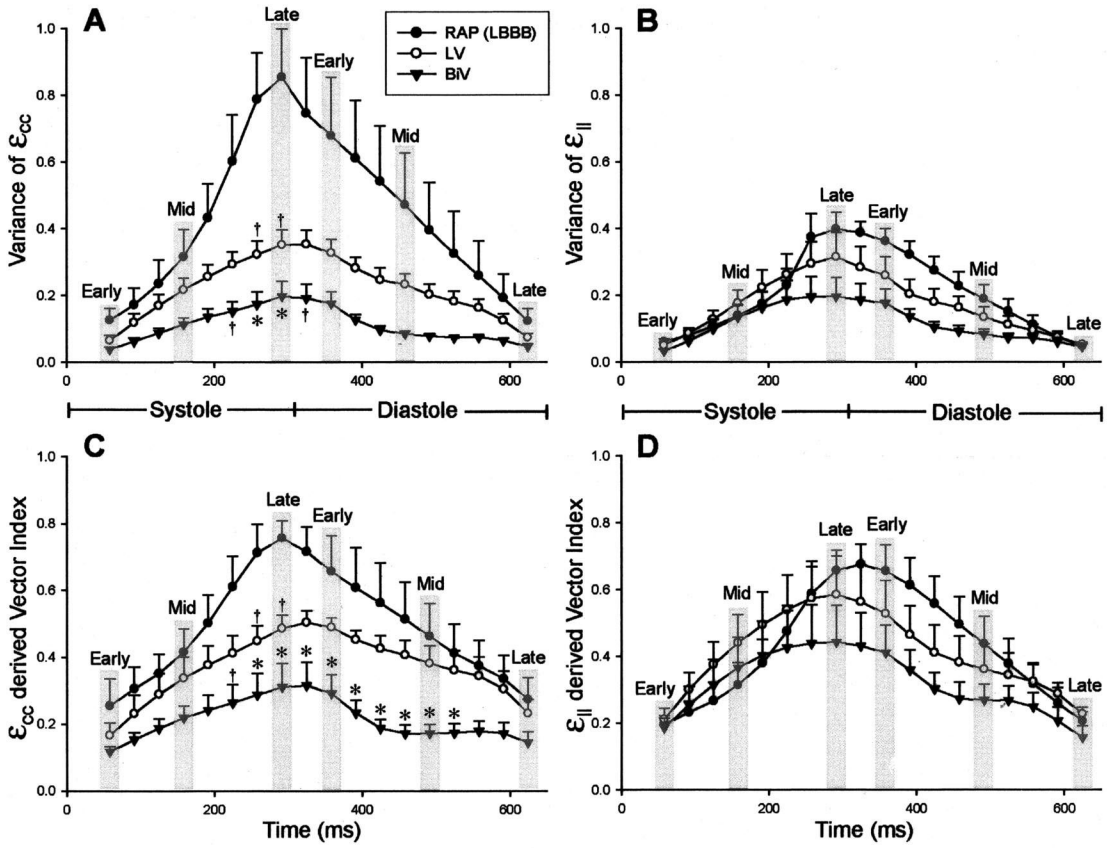

Figure 4.

Time-dependent plots of cardiac dyssynchrony and resolution of dyssynchrony based on analysis of ε_{cc} and ε_{ll} variance (A, B) and spatially weighted strain disparities (C, D). The strain variance rises (more dyssynchrony) and peaks at late systole and early diastole. For each pacing mode, LV and BiV are compared with RA (dyssynchronous) pacing at early, mid, and late time points in both systole and diastole (gray highlight). The time-dependent spatially weighed vector index (RVVPS) is also displayed for ε_{cc} and ε_{ll} (C, D). *P<0.009, †P<0.05 vs dyssynchronous (RA pacing, LBBB) baseline.

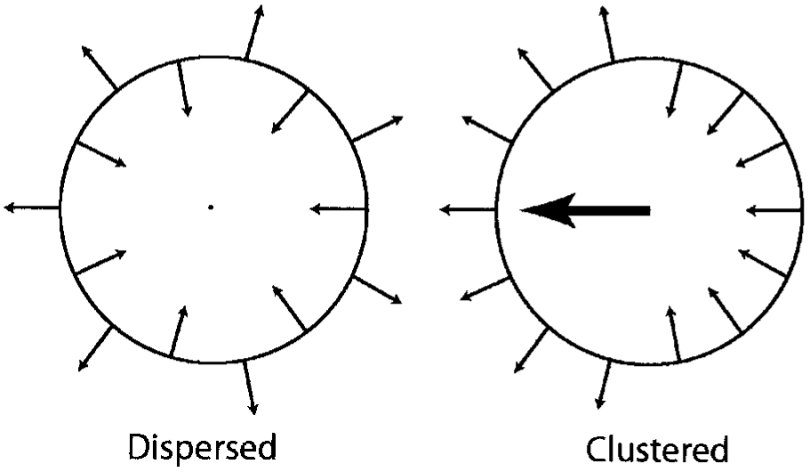

Figure 5.

Schematic of difference in net dyssynchrony based on geographic distribution of regions of delayed activation. When regions are locally clustered, the net impact on dysfunction is greater, whereas if they are dispersed throughout the wall, the impact is less. Importantly, both situations could result in similar numbers of delayed segments overall (counting dyssynchrony indexes) and similar variance of the delays. In contrast, a vector index would be zero for dispersed discoordinate shortening but non-zero when discoordinate motion was geographically clustered.